

Fission fragment angular distributions for neutron fission of ^{230}Th

J. W. Boldeman

*Australian Atomic Energy Commission Research Establishment, Private Mailbag, Sutherland, N.S.W. Australia
and Service de Physique Neutronique et Nucléaire, Centre d'Etudes de Bruyères-le-Châtel, 92542 Montrouge Cedex, France*

D. Gogny

Service de Physique Neutronique et Nucléaire, Centre d'Etudes de Bruyères-le-Châtel, 92542 Montrouge Cedex, France

A. R. de L. Musgrove and R. L. Walsh

Australian Atomic Energy Commission Research Establishment, Private Mailbag, Sutherland, N.S.W. Australia

(Received 4 February 1980)

Fission fragment angular distributions have been measured for the neutron fission of ^{230}Th in the energy range 680–1100 keV with special attention to the region of the large vibrational resonance in the neutron fission cross section near 715 keV. The analysis involved the search for a set of fission barrier parameters which lead to a simultaneous description of the angular distribution data and the existing data for the fission cross section. It was found that the data for the 715 keV resonance could be reproduced only if the $K = 1/2$ band responsible for this resonance splits into two separate bands, one of each parity, and if the decoupling parameter has a parity dependent sign. The derived moment of inertia constant $\hbar^2/2\mathcal{J}$ has a value of 1.85 keV which suggests that the vibrational resonance occurs within a minimum in the potential energy surface corresponding to a β deformation of $\epsilon_2 = 0.85$. The derived data are all consistent with the predicted triple-humped fission barrier for the thorium nuclei.

[NUCLEAR REACTIONS $^{230}\text{Th}(n, f)$, $E_n = 0.68 - 1.10$ MeV, measured $W(\theta)$, comprehensive statistical model analysis, barrier parameter derived, triple-humped fission barrier for thorium confirmed.]

I. INTRODUCTION

One of the more intriguing problems in fission at the present time is the shape of the potential energy surface for nuclei near thorium. Specifically the question is: Do the low lying fission barriers in this region have the more normal double-humped shape or have they a triple-humped shape as predicted¹ recently. The fact that there existed a problem first became apparent following attempts to explain the fission fragment angular distribution data of James *et al.*² and Yuen *et al.*³ To explain the angular distribution data and the neutron fission cross section² for ^{230}Th in the vicinity of the large subthreshold resonance at 715 keV, both groups were obliged to use a double-humped fission barrier in which the 715 keV resonance resulted from a pure vibrational resonance within a very shallow second minimum. The shape of the deduced barrier, two peaks of similar height separated by a shallow well, was very different from the shapes that were calculated for thorium at that time. For example, the barriers for thorium obtained by Pauli and Ledergerber⁴ had an inner barrier approximately 3 MeV lower in height. As the barrier shapes calculated for the uranium and plutonium nuclei were generally in agreement with experimental data to with-

in about 1 MeV, the serious discrepancy for thorium caused some concern and was labeled "the thorium anomaly."

A possible solution to this problem was suggested by Möller and Nix.¹ They showed that if mass asymmetric deformations were considered in the evaluation of the potential energy surfaces then, for the thorium isotopes, the outer peak of the usual double-humped shape splits into two separate peaks of similar height separated by a fairly shallow minimum. It was suggested that the vibrational state observed in experiment was situated within this third minimum.

The first experimental data to provide support for this hypothesis were the measurements of the neutron fission cross section of ^{232}Th by Blons *et al.*^{5,6} They observed multiple fine structures superimposed on the previously observed gross structure of the subthreshold cross section. The fine structures were interpreted as being due to rotational members of a pure vibrational state in the third minimum of a triple-humped fission barrier. It was argued that the vibrational state belonged to the third minimum because the moment of inertia constant $\hbar^2/2\mathcal{J}$ derived from the spacing of the members of the band was anomalously small and consistent with a deformation corresponding to that for a third minimum. However, a recent

measurement of the neutron fission cross section by Plattard *et al.*⁷ with similar resolution and statistical accuracy failed to confirm the details of the fine structure, without entirely excluding the existence of the type of structure seen by Blons *et al.*

The structure present in the neutron fission cross section of ^{230}Th is less complex than that for ^{232}Th and consequently a detailed study of this cross section should prove to be less ambiguous. Blons *et al.*⁸ have recently made this measurement, paying particular attention to the region near the large sub-barrier resonance at 715 keV. They claimed to have identified up to eight separate peaks superimposed on this resonance. The number of separate peaks in this analysis was crucial because the third minimum is predicted to occur for a mass asymmetric deformation. Because of the tunneling from one asymmetric shape to its inverse the quantum number K describing the projection of the total spin on the symmetric axis does not have parity. Thus, for example, a $K = \frac{1}{2}$ vibration resonance within the third minimum has effectively both positive and negative parity. The observation, therefore, of eight separate peaks ($g \leq \pm \frac{7}{2}$) could be adduced as proof of a triple-humped fission barrier.

Our previous contribution⁹ to this issue consisted of measurements of the fission fragment angular distributions for neutron fission of ^{232}Th in the energy region covered by the Blons *et al.* cross section measurements. In the analysis, a simultaneous description, using the calculation¹⁰ originally devised to explain fine structure in $\bar{\nu}_p$ and \bar{E}_K , was sought for all cross sections including the fission cross section and the fission fragment angular distributions. With barrier parameters consistent with those for a triple-humped barrier (i.e., a very shallow third minimum), a simultaneous description was possible of the gross structure in the fission cross section and the angular distributions. However, it was not possible to reproduce the fine structure seen by Blons *et al.* To reproduce the absolute magnitude of the fission cross section, the barrier parameters were such that, even without any damping in the third well, the FWHM of the partial cross section through any $IK\pi$ channel was of the order of 70 keV. Thus, structures with FWHM of 7 keV cannot be identified with members of such a rotational band. Recently, the earlier analysis has been extended to lower neutron energies without any significant modification of this conclusion. A similar analysis¹¹ of the ^{232}Th data at Bruyères-le-Châtel also supports this view.

It was clear from the fission fragment angular

distribution measurements for neutron fission of ^{232}Th that such data provide a very sensitive test of any proposed model. Consequently, measurements have been made of the fission fragment angular distributions for neutron fission of ^{230}Th from 680 to 1100 keV.

II. EXPERIMENTAL DETAILS

The experimental system was that described in Ref. 9 and is shown schematically in Fig. 1. Fragment detection was achieved with surface barrier detectors, whereas the two previous measurements for ^{230}Th (Refs. 2 and 3) used macro-foil. Conventional electronics were used with six separate pulse height analyzers. The ^{230}Th target was enriched to 99.85%. The average angle for each detector was computed using a Monte Carlo calculation which employed the exact geometry of the system. Corrections were applied for the nonuniform flux distribution across the target and for the laboratory to center of mass solid angle reduction. Neutrons were produced using analyzed protons from a 3 MeV Van de Graaff accelerator and the $^7\text{Li}(p,n)$ reaction.

III. RESULTS

The experimental fission fragment angular distributions are shown in Fig. 2. The accuracies are purely statistical. In the vicinity of the peak at 715 keV the energy resolution was ± 4 keV. At other energies the resolution was ± 8 keV. It was vital to ensure that the neutron energies used were reliable. One check was to ensure that the relative fission rates across the 715 keV resonance were consistent with the cross section measurements. It is estimated that the actual energies were accurate to within 3 keV.

The present data can be compared directly with the data of Yuen *et al.*³ at 680, 715, and 730 keV. At these energies, measurements were made with comparable energy resolution in the two experiments. The agreement between the two measurements is very good for the data at 680 and

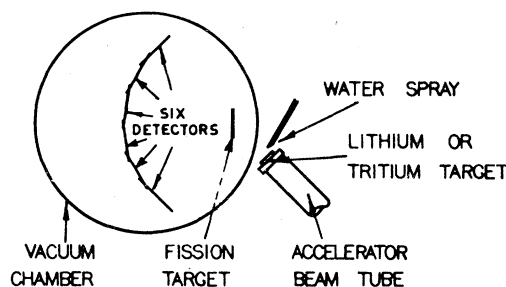


FIG. 1. Experimental system.

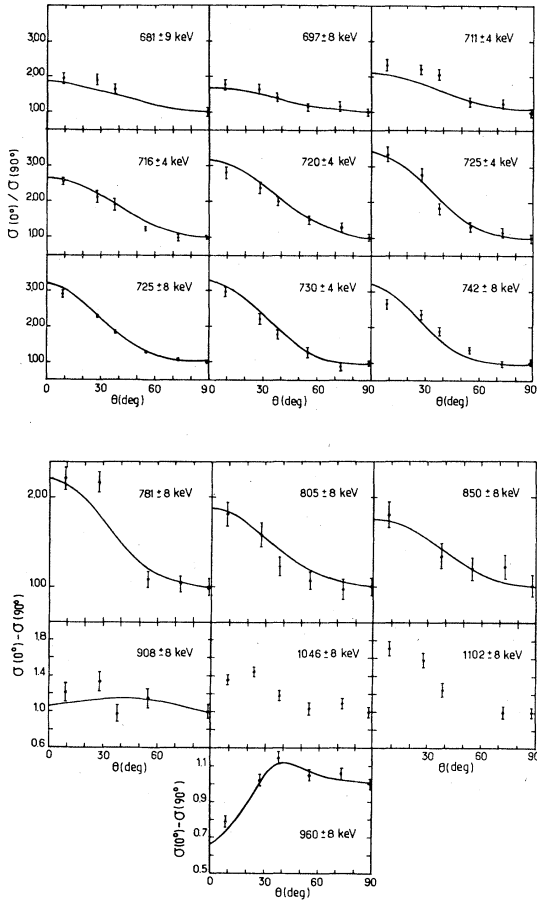


FIG. 2. Fission fragment angular distributions. The lines are the calculated angular distributions using the barrier parameters of Table III, weighted according to the fission cross section within the energy resolution.

730 keV. However, at 715 keV (and also at 711 keV) the present measurement shows more forward peaking. In this energy region the angular distribution is changing quite rapidly and to avoid such a difference as observed requires an accuracy in the energy probably better than that achieved in either experiment.

The anisotropy $[\sigma(0^\circ)/\sigma(90^\circ)]$ is shown for the data in the range 0.68–0.78 MeV in Fig. 3 and for the energy range 0.68–1.10 MeV in Fig. 4. The data from James *et al.*² for the 715 keV resonance have an energy resolution larger than the energy region over which the anisotropy is changing fairly rapidly. Consequently, the comparison for their data should be with a fission cross section weighted average. Recently, Leroux *et al.*¹² have also measured the fission fragment angular distributions for energies near 715 keV and the anisotropies from their measurement are also shown in Fig. 3. Generally the

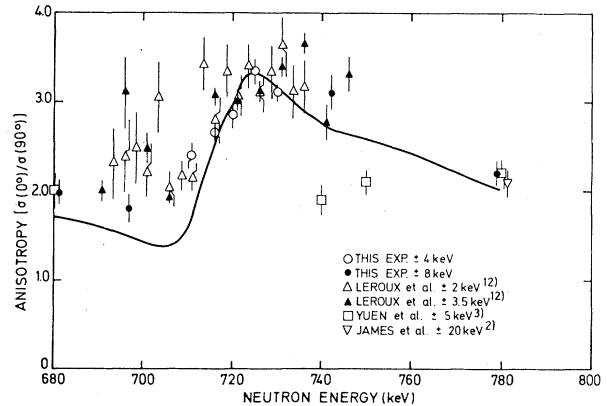


FIG. 3. Fission fragment anisotropy, $E_n = 680\text{--}800$ keV. The anisotropy calculated using the barrier parameters of Table II is also shown.

measured anisotropies from the different measurements across the peak are in reasonable agreement. Below the peak there is a suggestion of a small peak in the anisotropy near 700 keV from the data of Leroux *et al.* which is not supported by the present work.

IV. METHOD OF ANALYSIS

The analysis followed the method given in the previous paper on ²³²Th (Ref. 9) and was based on the statistical model.¹³ The capture of an incident neutron with energy E_n by the target ²³⁰Th leads to the formation of a compound nucleus which subsequently decays by neutron emission, gamma ray emission, or fission. The various cross sections may be written in the form

$$\sigma_{cc'}(E_n) = \sum_{I\pi} \sigma_c(E, I, \pi) P_{c'}(E, I, \pi), \quad (1)$$

where c and c' label the entrance and exit chan-

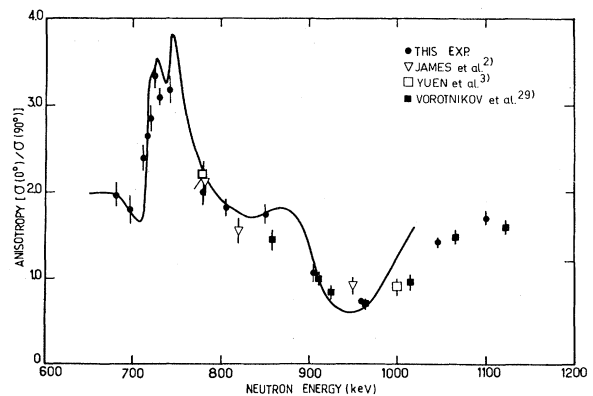


FIG. 4. Fission fragment anisotropy, $E_n = 680\text{--}1100$ keV. The anisotropy calculated using the barrier parameters of Table III is also shown.

nels, respectively, $\sigma_c(E, I, \pi)$ is the cross section for formation of the compound nucleus state with total angular momentum I and parity π at the excitation energy E , and $P_{c'}$ is the branching ratio to the channel c' with corrections due to width fluctuations. Thus, the cross section for neutron emission to a final state λ of the target nucleus is given by

$$\sigma_{n, n'}(\lambda) = \sum \sigma_c(E, I, \pi) \frac{T_n(E - E_\lambda, I, \pi) F_{n, n'}}{T_f^t + T_n^t + T_\gamma^t}, \quad (2)$$

where T_n , T_f , and T_γ denote the transmission coefficients for neutron emission, fission and radiative capture, respectively, and the superscript t signifies summation over all channels for each mode. $F_{n, n'}$ is a level width fluctuation factor. Similar expressions can be written for the fission and capture cross sections.

The neutron transmission coefficients were calculated using the optical model potential of Moldauer,¹⁴ which, although it is a spherical potential, does reproduce the experimental s and p wave strength functions in this mass region. The fluctuation corrections were based on a combination of the methods of Hofmann *et al.*¹⁵ and Bertram.¹⁶ The radiative capture transmission coefficient T_γ is related to the average capture width $\bar{\Gamma}_\gamma$ by

$$T_\gamma(E, I, \pi) = 2\pi\rho(E, I, \pi) \bar{\Gamma}_\gamma(E), \quad (3)$$

where $\rho(E, I, \pi)$ denotes the Fermi-gas level density of the compound nucleus ²³³Th. The γ ray widths were calculated according to the Weiskopf formalism¹⁷ and normalized to the measured average radiative width in the resolved resonance region. For the evaluation of the fission penetrabilities the fission barriers were parametrized by smoothly joined parabolas following the procedure of Cramer and Nix.¹⁸ The penetrabilities were obtained from an exact solution of the Schrödinger equation. The differential fission cross section is given by

$$\langle \sigma_f(E_n, \theta) \rangle = \sum_{IK\pi} \sigma_f^{IK\pi}(E_n) W_{IK}(\theta), \quad (4)$$

where the quantum numbers $IK\pi$ specify the particular fission channel. K is the projection of the total angular momentum I on the symmetry axis of the nucleus. The fission fragment angular distribution $W_{IK}(\theta)$ for fission through each channel IK is given by

$$W_{IK}(\theta) = \frac{1}{4}(2I+1) [|d_{1/2, K}(\theta)|^2 + |d_{-1/2, K}(\theta)|^2], \quad (5)$$

where $|d|^2$ is the square of the rotational part of the symmetric-top wave function.¹⁹

For an odd-mass compound nucleus such as

²³¹Th the lowest lying fission channels are expected to be essentially single particle states which should be identifiable with the appropriate Nilsson orbits. The excess angular momentum appears as a rotation about an axis perpendicular to the symmetric axis. Thus, with each intrinsic state there is associated a rotational band with energies given by

$$E(I^\pi) = E_0 + \frac{\hbar^2}{2\mathcal{I}} [I(I+1) - 2K^2 + \delta_{K, 1/2} \alpha (-1)^{I+1/2} (I+1/2)], \quad (6)$$

where \mathcal{I} is the moment of inertia associated with the band and α is the decoupling constant for the $K = \frac{1}{2}$ bands. For a particular band, the fission barriers are assumed to be identical in shape and merely displaced with respect to each other according to Eq. (6).

The analytical procedure involved the search for a set of fission barriers which led to calculated cross sections consistent with all the experimental data. In particular, it was considered essential to reproduce simultaneously the neutron fission cross section and the angular distributions.

There is a large number of free parameters in the analysis and consequently some criticism might be leveled at the reliability of the conclusions drawn. To reduce as much as possible any criticism on this score the entire analysis was repeated at Bruyères-le-Châtel with the code NRLY (J. Jary, unpublished), hereafter designated BRC. The philosophy of this code is the same as above but many of the details are completely different. For example, the transmission coefficients were those of Lagrange²⁰ derived from a coupled channel analysis of neutron data in this mass region. The fluctuation corrections were also calculated differently. The two methods of analysis have been compared in detail for ²³²Th in Ref. 11. As in that case it was found that they lead to almost identical fission barriers.

V. RESULTS OF THE ANALYSIS

The constant input data are listed in Table I. Before discussing the results of the analysis, there are several points to emphasize. The object of the analysis was to demonstrate that the lowest lying barriers for ²³⁰Th have a triple-humped shape. As pointed out previously, there are three possible features of the analysis which would be consistent with this hypothesis.

(i) The triple-humped barrier is itself predicted by the analysis. Unfortunately, it is apparent that this cannot be the case. The inner peak of the triple-humped barrier, if it exists, is very much lower in height than the outer two peaks.

TABLE I. Constant input data.

Inelastic scattering levels (MeV)	Spin
0.0532	2 ⁺
0.174	4 ⁺
0.357	6 ⁺
0.508	1 ⁻
0.572	3 ⁻
0.582	8 ⁺
0.635	0 ⁺
0.678	2 ⁺
0.682	5 ⁻
0.781	2 ⁺
0.826	3 ⁺

$$\frac{\Gamma_\gamma}{D} (\text{resonance region}) = \frac{18 \text{ meV}}{7 \text{ eV}}$$

Consequently, only the heights of the outer two peaks will influence the fission cross section and the angular distributions. Thus, the most that can be derived from the analyzed shape of the barrier is that the shape of the outer two peaks is consistent with the predicted triple-humped shape. This conclusion can be drawn already from the two earliest analyses.^{2,3}

(ii) The moment of inertia constant ($\hbar^2/2\mathcal{I}$) in the expression for the rotational band has typically a value of ≈ 7 keV for uranium and thorium nuclei in their ground state, i.e., in the first well of the fission barrier. According to Metag,²¹ the moment of inertia constant for fission isomers in the second well is typically 3.3 keV. Thus a moment of inertia constant significantly smaller would indicate a larger deformation and therefore be consistent with the proposed triple-humped barrier. This was the essence of the argument of Blons *et al.*⁵ but Abou Yehia *et al.*¹¹ in a more elaborate analysis were unable to confirm this conclusion for ²³²Th.

(iii) The unambiguous identification of rotational bands of both parities for a specific vibrational resonance would provide clear proof of a mass asymmetric minimum.

For convenience, the analysis of the ²³⁰Th data is best divided into two parts: the resonance at 715 keV (Sec. VA) and the data at higher energies (Sec. VA2).

A. Analysis below 780 keV

The cross section in the region below 780 keV is dominated by the cross section associated with the band(s) giving rise to the resonance at 715 keV and, in fact, the minimum in the cross section at 780 keV is so low that in this region the tails of the partial cross sections associated with the higher barriers can be neglected to a first

approximation. The primary objective of the analysis was therefore to distinguish between the possibilities of fitting the data with a rotational band of single parity and of fitting the data with two rotational bands, one of each parity.

1. Single parity option

A very extensive search was made using both codes to find a set of parameters which would accurately reproduce all experimental data. The best compromise fit to the experimental data was that obtained using the barrier parameters given in Table II (actual parameters from L. H. code). In this search, negative parity for the $K=\frac{1}{2}$ band was quickly eliminated. The energy dependence of the fission fragment anisotropy calculated with the parameters of Table II is shown with the experimental data in Fig. 3. In Fig. 5, the calculated fission cross section is shown with the data of Blons *et al.*⁸

The calculated anisotropies are in very good agreement with the experimental data with only a minor problem in the energy region near 700 keV where measurements are difficult to make and where there is also some disagreement within the data. However, the calculated cross section is at best a poor reproduction of the experimental data. Since a very large number of cases was tried, it is extremely unlikely that a better set of parameters has been overlooked.

Three possible explanations can be advanced for the failure of the single parity option to provide a completely satisfactory fit to all experimental data. The first two have been discussed in detail by Lynn *et al.*²²

(i) The input data and, in particular, the transmission coefficients are in error.

(ii) The fission barriers, e.g., E_c , $\hbar\omega_c$ vary for different rotational members of the band.

(iii) Both parities are required.

(i) Both calculations (L. H. and BRC) gave almost identical magnitudes for the various partial cross sections. The transmission coefficients also produced strength functions of $S_0=1 \times 10^{-4}$, $S_1=1.6 \times 10^{-4}$, and $S_2=1 \times 10^{-4}$ in the resolved region, which are consistent with the experimental data. In addition, the transmission coefficients from Lagrange were derived from a comprehensive fit to all existing neutron data for the thorium and uranium nuclei. However, even substantial

TABLE II. Barrier parameters for single parity fit (MeV). $K=\frac{1}{2}^+$; $\hbar^2/2\mathcal{I}=1.8$ keV; $\alpha=0$.

E_B	E_{III}	E_c	$\hbar\omega_B$	$\hbar\omega_{III}$	$\hbar\omega_c$
6.30	5.585	6.360	1.300	0.510	0.850

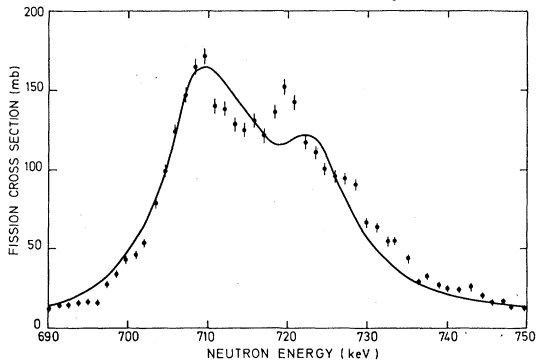


FIG. 5. The fission cross section calculated using the parameters of Table II. Data of Blons *et al.* (Ref. 8) are shown.

changes in the input data do not significantly improve the fit to the experimental data. For example, an increase in the d -wave cross section by about 50% can increase the $I = \frac{5}{2}^+$ peak near 720 keV but leads to a worsening of the fit near the $I = \frac{3}{2}^+$ peak (715 keV). A shift of the $\frac{3}{2}^+$ peak downwards in energy (by reducing $\hbar^2/2\mathcal{I}$ for example) improves the fit near the two major peaks of the cross section but leads to severe difficulties above 725 keV. Consequently, the possibility of error in the transmission coefficients as the cause of the disagreement with the experimental data can probably be dismissed.

(ii) In this calculation and generally in calculations of this type it was assumed that the fission barriers for the members of each rotational band were identical in shape and merely displaced at all deformations according to Eq. (6). There are two ways whereby this may not be the case. Firstly, there is the possibility of Coriolis coupling between states with the same I but belonging to rotational bands differing in K by a unit of angular momentum. The present analysis was extended to much higher energy (see Sec. VB). The next highest rotational band was found to have $K = \frac{3}{2}$ (see Table III for the band structure in the double parity fit). In an overall single parity fit, the $K^\pi = \frac{1}{2}^+$ and $K = \frac{3}{2}$ bands are well separated except at the second outer peak of the barrier (the lower of the two peaks). The effect of the Coriolis coupling between the two bands would be to reduce slightly the $K^\pi = \frac{1}{2}^+$, $I^\pi = \frac{3}{2}^+$, $\frac{5}{2}^+$... partial cross sections and also to broaden their resonance peaks. This would lead to a deterioration in the quality of the fit to the experimental data and cannot be the answer to the problem. Secondly, in the Nilsson picture, the intrinsic states are components of rotational bands with single particle orbitals as the band heads. The relative position in energy of the peaks of the partial cross sections

TABLE III. Barrier parameters for double parity fit (MeV). $\hbar^2/2\mathcal{I} = 1.85$ keV, $\alpha = -1.1$ positive parity, $\alpha = +1.1$ negative parity.

K^π	E_B	E_{III}	E_C	$\hbar\omega_B$	$\hbar\omega_{III}$	$\hbar\omega_C$
$\frac{1}{2}^+$	6.068	5.585	6.339	0.60	0.51	0.70
$\frac{1}{2}^-$	6.071	5.588	6.342	0.60	0.51	0.70
$\frac{1}{2}^-$	6.010	5.745	6.490	0.75	0.51	0.65
$\frac{3}{2}^+$	6.050	5.700	6.490	0.60	0.95	0.73
$\frac{3}{2}^-$	6.080	5.730	6.520	0.60	0.95	0.73
$\frac{1}{2}^-$	6.185	5.795	6.530	0.60	1.00	0.70
$\frac{1}{2}^+$	6.205	5.815	6.550	0.60	1.00	0.70

contributing to the resonance at 715 keV are determined by the rotational band structure at the deformation corresponding to that particular minimum in the potential energy surface. The relative magnitudes, however, are determined by the barrier shapes at other deformations, particularly those in the vicinity of the outer peak. As stated previously, these shapes were assumed to be the same. If, however, at these other deformations crossings occur of other single particle orbits, then mixing will take place leading to modification of the barrier shape. This possibility can also be discarded on reasonable grounds. These crossings are rather infrequent and the calculated single particle levels²³ do not show such crossings at the deformation where such behavior would be most significant, i.e., the outer peak. Furthermore, crossings of $I^\pi = \frac{3}{2}^+$ and $\frac{5}{2}^+$ orbitals are required to produce the required effect and of course the $I = \frac{3}{2}$ levels are shielded by the next highest $K = \frac{3}{2}$ bands.

(iii) The only explanation that remains to explain the failure to achieve a suitable fit to the data is the requirement of both parities for the rotational members of the band.

2. Double parity option

Blons *et al.*⁸ were the first to realize that the $K = \frac{1}{2}$ vibrational level responsible for the resonance at 715 keV should split into two separate rotational bands of each parity if the minimum in the potential energy surface was caused by a mass asymmetric deformation. To recognize all the implications of this possibility it is necessary to elucidate the underlying details.

The Hamiltonian separating the intrinsic and rotational degrees of freedom has the form

$$H = H_{\text{intr}}(q, p, \epsilon_2, \epsilon_3) + H_{\text{rot}, \alpha}(P_\omega), \quad (7)$$

where the intrinsic motion is described by the

coordinates q and conjugate momenta p and the rotational component does not depend on the orientation ω , but is a function of the conjugate angular momenta P_ω . ϵ_2 describes the quadrupole deformation and ϵ_3 the mass asymmetry (Fig. 6) where it is assumed that rotational motion and collective motion associated with the collective degrees of freedom (ϵ_2 , ϵ_3) are decoupled. The eigenstates (α) of the Hamiltonian are given by

$$\psi_{\alpha,I} = \Phi_\alpha(q, \epsilon_2, \epsilon_3) \varphi_{\alpha,I}(\omega). \quad (8)$$

For specific values of the three quantum numbers I , K , and M the rotational wave function is

$$\varphi_{IKM}(\omega) = \left(\frac{2I+1}{8\pi^2} \right)^{1/2} \mathcal{D}_{MK}^I(\omega). \quad (9)$$

In general the intrinsic Hamiltonian is invariant with respect to a rotation of 180° $R_y(\pi)$ about an axis perpendicular to the symmetric axis and the nuclear wave function has the form²⁴

$$\psi_{IKM} = \left(\frac{2I+1}{16\pi^2} \right)^{1/2} [\Phi_K(q) \mathcal{D}_{MK}^I(\omega) + (-1)^{I+K} \Phi_{\bar{K}}(q) \mathcal{D}_{M-K}^I(\omega)], \quad (10)$$

$$I = K, K+1, \dots \text{ for } K > 0$$

where the bar on the K signifies the time reversed intrinsic state. If, however, the dynamic associated with the mass asymmetric degree of freedom is considered, characterized by the values of ϵ_3 , it implies a violation of reflection symmetry and the system acquires a doublet structure containing all values of $I \geq |K|$, i.e., both parities. Now the intrinsic state is given by two combinations of two intrinsic states of opposite asymmetry:

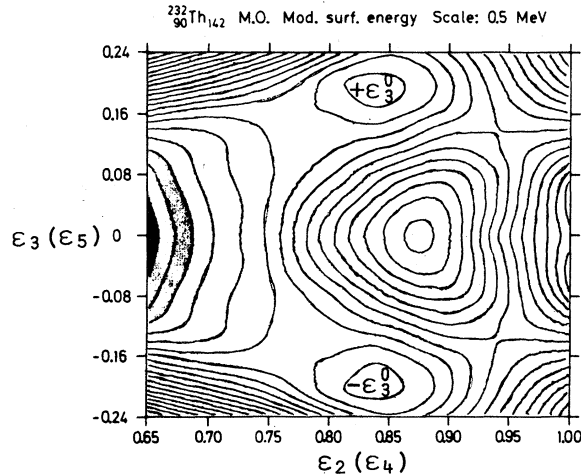


FIG. 6. Potential energy surface as function of coordinates ϵ_2 , ϵ_3 , from Ref. 23.

$$\Phi_K^\pi = \frac{1}{\sqrt{2}} [\Phi(\epsilon_3^0, q) \pm \Phi(-\epsilon_3^0, q)], \quad (11)$$

where ϵ_3^0 and $-\epsilon_3^0$ denote the positions of the two asymmetric wells for a frozen value of ϵ_2 . The law of transformation of these two intrinsic parity states Φ_K^π with respect to $R_y(\pi)$ is given by

$$\begin{aligned} R_y(\pi) \Phi_K^+ &= +\Phi_K^+, \\ R_y(\pi) \Phi_K^- &= -\Phi_K^-. \end{aligned} \quad (12)$$

Accordingly, the nuclear wave function becomes²⁴

$$\begin{aligned} \psi_{IKM}^\pi &= \left(\frac{2I+1}{16\pi^2} \right)^{1/2} [\Phi_K \mathcal{D}_{MK}^I + (-1)^{I+K} \Phi_{\bar{K}} \mathcal{D}_{M-K}^I], \quad \pi = +1 \\ &= \left(\frac{2I+1}{16\pi^2} \right)^{1/2} i [\Phi_K \mathcal{D}_{MK}^I - (-1)^{I+K} \Phi_{\bar{K}} \mathcal{D}_{M-K}^I], \quad \pi = -1. \end{aligned} \quad (13)$$

The energy spectrum in this model can be expressed as follows taking into account the Coriolis coupling of the odd particle with the core:

$$\begin{aligned} E_{IKM}^\pi &= \xi_K^\pi + \frac{\hbar^2}{2\mathcal{J}} [I(I+1) - 2K^2] \\ &\quad - \frac{\hbar^2}{2\mathcal{J}} \langle \pi IKM | I_+ j_- + I_- j_+ | \pi IKM \rangle. \end{aligned} \quad (14)$$

The difference ($\xi_K^+ - \xi_K^-$) between the two intrinsic energies is given by the tunneling through the barrier separating the two wells. The Coriolis coupling contribution can be written in the usual form

$$\alpha^\pi \frac{\hbar^2}{2\mathcal{J}} (I+1/2) \delta_{K, 1/2} (-1)^{I+1/2}, \quad (15)$$

where α^π is the so called decoupling parameter which can be written in this case as

$$\alpha^+ = -\langle \Phi_K^+ | j_+ | \Phi_{\bar{K}}^+ \rangle, \quad \alpha^- = \langle \Phi_K^- | j_+ | \Phi_{\bar{K}}^- \rangle. \quad (16)$$

With the help of Eq. (11), it is seen that the magnitude of both is approximately the same if it is assumed that there is little overlap of the two intrinsic wave functions in the separate well, i.e., $\langle \Phi(\epsilon_3^0, q) | \Phi(-\epsilon_3^0, q) \rangle \ll 1$. However, it should be emphasized that the signs are different.

For the double parity option, it is obvious that there is a large number of parameters involved and that to facilitate a meaningful analysis it is necessary to reduce their number. This was achieved as follows. The barrier parameters ($E_B, E_{III}, E_c, \hbar\omega_B, \hbar\omega_{III}, \hbar\omega_c$) were set by the following three requirements: (a) The total area of the resonance had to be reproduced; (b) the FWHM of all partial cross sections was 10 keV, and (c) the third minimum corresponded to a β deformation of $\epsilon_2 = 0.85$. This operation then left three adjustable parameters with which to achieve a comprehensive fit, i.e., ΔE the separation of the

+ve and -ve parity components of the resonance, $\hbar^2/2\mathcal{I}$ the moment of inertia constant, and α the decoupling parameter (one sign for the positive parity band; the other for the negative parity band). In fact it was a fairly simple matter to find a very satisfactory solution. The first part of Table III lists all the parameters for this fit. The calculated fission cross section is shown in comparison with the experimental data in Fig. 7. In Fig. 8 the calculated energy dependence of the anisotropy is shown with experimental data. The actual parameters given in Table III were those employed in the final BRC calculation. The L. H. calculation produced almost identical values with only a minor adjustment of the outer peak heights. The input neutron parameters were not varied in any way apart from a reduction of 40% in the f -wave transmission coefficients. In the L.H. calculation an equivalent fit to the cross section was obtained by using an f -wave strength function of 1.2×10^{-4} . This modification is reasonable and does not affect the comprehensive fit to neutron data in this mass region.²⁰

The calculated fission cross section is in very good agreement with the experimental data with all statistically significant features being reproduced. The calculation also reproduces the anisotropy data very well with only few areas of apparent disagreement. The most serious disagreement appears to be at 745 keV where the calculation gives rise to a narrow peak in the anisotropy. The present measurement near that energy (742 keV) was made with ± 8 keV energy resolution. The more precise comparison, therefore, is with the calculated angular distribution weighted according to the fission cross section within the neutron energy resolution. The lines shown in Fig. 2 with the experimental data have

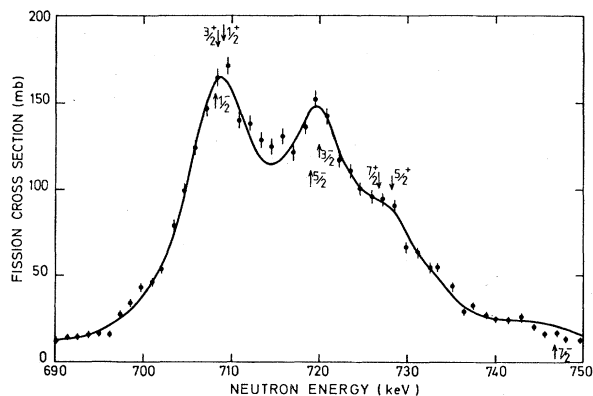


FIG. 7. The fission cross section calculated using the parameters of Table III. Data of Blons *et al.* (Ref. 8) are shown.

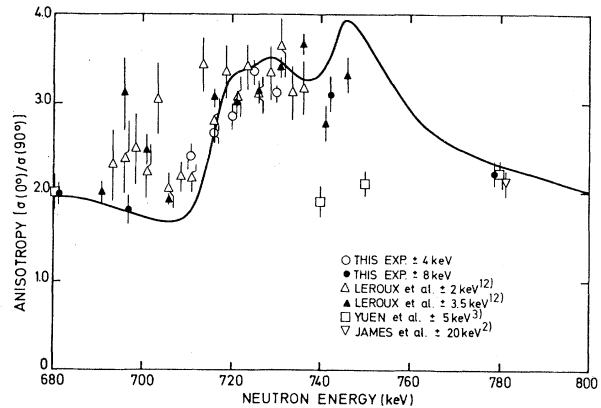


FIG. 8. The fission fragment anisotropy calculated using the parameters of Table III.

been calculated in this way. For the data at 742 ± 8 keV, the agreement with calculation is now seen to be very much better. In fact, the agreement between experiment and calculation is found to be generally better in Fig. 2 than that suggested by the anisotropy comparison in Fig. 8 which gives the unbroadened calculation only.

Since the simultaneous fit to all experimental data is so reasonable, it is important to determine whether this fit is in any way unique. In the preliminary analysis of this experiment,²⁵ strong reservations were expressed as to whether an analysis of this kind could lead to unambiguous verification of the triple-humped barrier. The reason for this reservation was that a single parity fit (basically the fit in Table II, Figs. 3 and 5) was at least as reasonable as any fit produced with double parities. For example, the fission cross section and fission fragment anisotropies calculated using the scheme of Blons *et al.*⁸ ($\hbar^2/2\mathcal{I} = 1.9$ keV, $\Delta E = 10.8$ keV, and $\alpha = -2.28$ for both parities) and the present barriers are seen to be in only approximate agreement with the fission cross section in Fig. 9 and in disagreement with the angular distributions in Fig. 10. (Blons *et al.*²⁶ are also proceeding with a full analytical description of the ^{230}Th data using a decoupling parameter with parity dependent sign.) Subsequently, in attempts to improve the simultaneous fit to the data, also with the mistake of the same sign for the decoupling parameter, the only successful scheme utilized the parameters $\Delta E \approx 0$ keV, $\alpha = 3.34$, and $\hbar^2/2\mathcal{I} = 0.7$ keV. The value for the moment of inertia constant was uncomfortably small and much lower than physically reasonable limits.^{27,28} Of course, the problem in both of these cases was the use of the same sign for the decoupling parameter for the +ve and -ve

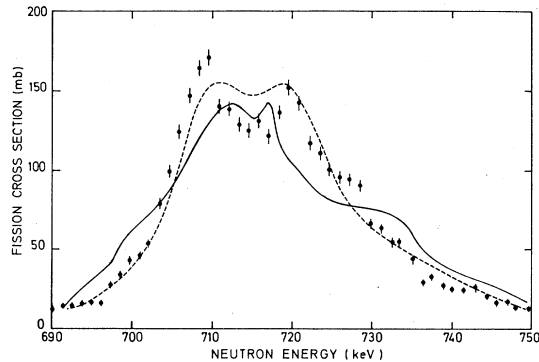


FIG. 9. Calculated fission cross section: — using the scheme $\hbar^2/2g=1.9$ keV, $\Delta E=10.8$ keV, $\alpha=-2.28$ for both parity bands; ---- using the scheme $\hbar^2/2g=0.7$ keV, $\Delta E \approx 0$ and $\alpha=3.34$ for both parity bands.

parity bands. However, these exercises serve to demonstrate the probable validity of the parameters in Table III.

A second scheme within this philosophy which provides not unreasonable fits to the data involves the exchange of all parameters for $+ve$ and $-ve$ parity bands. However, this scheme is very much inferior to the scheme of Table III and the detailed data are not presented.

B. Analysis above 780 keV

The analysis of the experimental data above 780 keV becomes much less reliable because of the rapid increase in the number of effective fission channels and because the quality of the angular distribution data is poorer. In such an analysis there are three features which should be reproduced.

(i) There is a small peak in the fission cross section at 850 keV which appears to be accompanied by some increase in the anisotropy al-

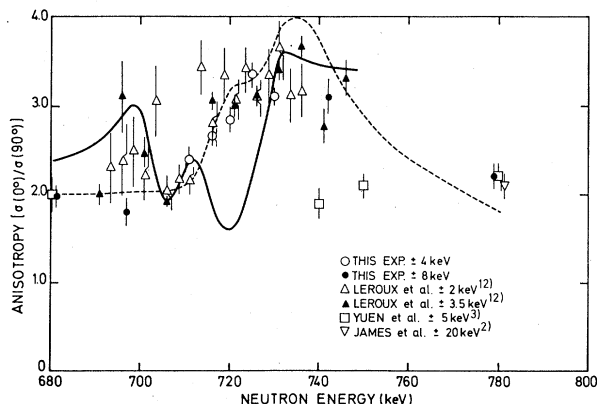


FIG. 10. Calculated fission fragment anisotropies. The lines have the same source as in Fig. 9.

though the data are rather sparse.

(ii) A very deep minimum occurs in the anisotropy at 950 keV but the cross section here shows only a shelf.

(iii) Above 1000 keV, the anisotropy becomes again forward peaked.

The complete set of barrier parameters listed in Table III reproduces most of these features. In Fig. 11, the calculated fission cross section is shown with the data of James *et al.*² and Blons *et al.*⁸ The data of James *et al.*² have not been plotted for the energy range below 975 keV as they show the effect of experimental resolution. The calculated anisotropies are shown with the experimental data in Fig. 4. There are a number of features to note.

(i) The peak at 850 keV can only be associated with a $K=\frac{1}{2}$ band. However, the resolution in the measurement of Blons *et al.* was sufficient to show that it is certainly not a fully developed vibrational resonance. The data in this region have been simulated by the third barrier in Table III. Such a barrier presents some problems as it might be expected to interfere with the ground state $K=\pm\frac{1}{2}$ bands at the second outer peak. Perhaps the failure to interfere with the ground state bands may be taken as evidence of an alternative path to fission. The structure at 850 keV could also be conceivably explained as another feature of the ground state cross section. In the analysis the barriers have been parametrized by smoothly joined parabolas. This is at best an approximation and the data at 850 keV could possibly be an indication of additional structure in the fission

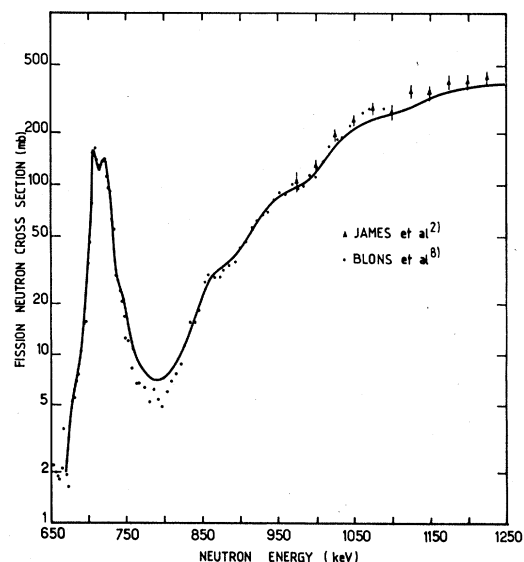


FIG. 11. Calculated fission cross section using the parameters of Table III.

barrier.

(ii) The strong but localized sideways peaking of the angular distribution near 950 keV is attributed to the strong influence at that energy of $K = \pm \frac{3}{2}$ bands (triple-humped barrier) for which the third minimum is too shallow to include a quasistationary state. The barrier shapes (barriers 4 and 5 in Table III) give rise to a broad maximum at 960 keV in the fission cross section. In the analysis some considerable effort was spent in an endeavor to find a solution with $K = \pm \frac{5}{2}$ assignments for these bands. However, no solution could be found which reproduced the shape of the angular distribution at 960 ± 8 keV. With $K = \pm \frac{3}{2}$ for these barriers, there is the possibility of Coriolis coupling with the $I = \pm \frac{3}{2}, \pm \frac{5}{2}, \dots$ members of $K = \pm \frac{1}{2}$ ground state bands. This would lead to some minor modifications of the band structures at the second outermost peak of the barrier but would have a negligible effect on the partial fission cross sections as these are dominated by the height and curvature of the outer peak.

(iii) Above 1000 keV, the final two fission barriers begin to contribute strongly. It is clear from the experimental data that strong components of $K = \frac{1}{2}$ bands are required between 1000 and 1100 keV. Barriers 6 and 7 provide that strength and may be reasonable approximations to the real barriers. Above 1050 keV it is apparent that barriers with $K \geq \frac{3}{2}$ become operative but it becomes a meaningless exercise to extend the analysis into this region.

VI. COMPARISON WITH CALCULATED SINGLE PARTICLE LEVELS

The level scheme derived from the present analysis can be compared with that calculated by Ragnarsson *et al.*²³ for $Z = 90$ (thorium). Figure 12 shows the single particle levels at a β deformation of $\epsilon_2 = 0.85$ for different values of the mass asymmetric parameter ϵ_3 . The third minimum in the potential energy surface is predicted to occur at $\epsilon_3 = 0.18$. Thus, there is a clearcut candidate for the role of the single particle band head of the $K = \frac{1}{2}$ band, namely, the $860 \frac{1}{2}^+$ level which is calculated to be near the Fermi surface for $N = 141$. The sign of the calculated decoupling parameter is not confirmed. The next two levels in the calculated scheme are $\frac{5}{2}$ and $\frac{3}{2}$. The present analysis points to a reversal of their positions.

VII. CONCLUSION

The evidence for a triple-humped fission barrier in the thorium region is now very persuasive and can be summarized as follows.

(1) It is a natural prediction of theory.

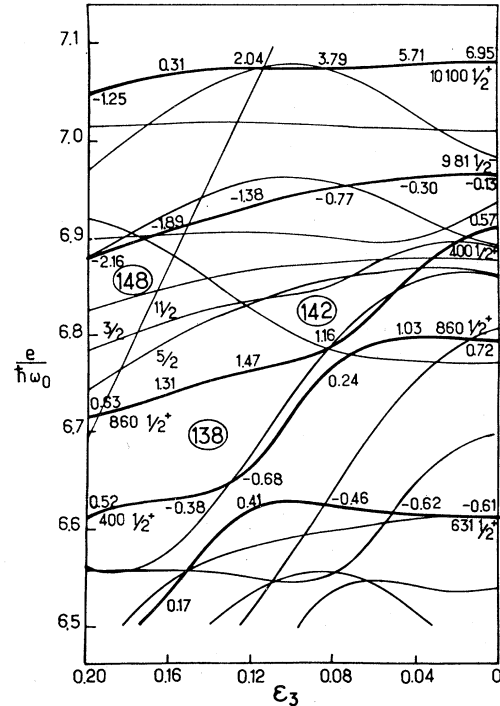


FIG. 12. Calculated single particle scheme from Ragnarsson *et al.* (Ref. 23) for $Z = 90$ and for $\epsilon_2 = 0.85$.

(2) All the barrier shapes derived in the present analysis of the ^{230}Th data had a similar shape, namely, two outer peaks of similar height separated by a shallow minimum. The predicted triple-humped fission barriers have such a shape.

(3) The data for the 715 keV resonance can be reproduced only when both parities are permitted for the $K = \frac{1}{2}$ band and only when the sign of the decoupling parameter is parity dependent.

(4) The moment of inertia constant derived in the analysis of the data has a value of 1.85 keV which is consistent with a β deformation of $\epsilon_2 = 0.85$ (Pauli and Ledergerber²⁷) which is the predicted deformation of the third minimum.

Further evidence for the triple-humped shape is desirable. It is clear that the fission fragment angular distribution data require improvement in addition to more extensive measurements near 850 keV neutron energy. Bhandari³⁰ has shown that a shape isomer in the second well of the triple-humped barrier should decay only by gamma ray emission with a half-life of approximately 100 nsec. An attempt to excite this state using the (d, p) reaction³¹ was unsuccessful because of the background, but further attempts should be made using a different reaction. There is in addition a need for a high resolution measurement of the $^{230}\text{Th}(d, p, f)$ cross section. A comparison of the resonance shape with that observed

in the (n, f) reaction would provide additional verification of the present findings.

ACKNOWLEDGMENTS

We wish to thank J. Jary for the use of her program (BRC). We also acknowledge illuminating

discussions with J. Blons, D. Paya, I. Ragnarsson, and G. Leander. We are also indebted to B. Leroux for the permission to quote his unpublished data. Finally, one of us (JWB) would like to thank the CEA for their hospitality during an attachment to Bruyères-le-Châtel.

- ¹P. Möller and R. Nix, *Proceedings of the Third IAEA Symposium on the Physics and Chemistry of Fission, Rochester 1973* (IAEA, Vienna, 1974), Vol. 1, p. 103.
- ²G. D. James, J. E. Lynn, and L. G. Earwaker, *Nucl. Phys.* **189**, 225 (1972).
- ³G. Yuen, G. T. Rizzo, A. N. Behkami, and J. R. Hui-zenga, *Nucl. Phys.* **171**, 614 (1971).
- ⁴H. C. Pauli and T. Ledergerber, *Nucl. Phys.* **175**, 545 (1971).
- ⁵J. Blons, C. Mazur, and D. Paya, *Phys. Rev. Lett.* **35**, 1749 (1975).
- ⁶J. Blons, C. Mazur, D. Paya, M. Ribrag, and H. Weig-mann, IAEA Symposium on the Physics and Chemistry of Fission, Jülich, 1979 (unpublished).
- ⁷S. Plattard, G. F. Auchampaugh, N. W. Hill, R. B. Perez, and G. de Saussure, IAEA Symposium on the Physics and Chemistry of Fission, Jülich, 1979 (un-published).
- ⁸J. Blons, C. Mazur, D. Paya, M. Ribrag, and H. Weig-mann, *Phys. Rev. Lett.* **41**, 1289 (1978).
- ⁹J. Caruana, J. W. Boldeman, and R. L. Walsh, *Nucl. Phys.* **285**, 205 (1977).
- ¹⁰J. W. Boldeman, W. K. Bertram, and R. L. Walsh, *Nucl. Phys.* **265**, 337 (1976).
- ¹¹H. Abou Yehia, J. Jary, J. Trochon, J. W. Boldeman, and A. R. de L. Musgrove, International Conference on Neutron Cross Sections for Technology, Knoxville, 1979 (to be published).
- ¹²B. Leroux, G. T. Barreau, A. Sicre, T. Benfoughal, F. Caitucoli, J. P. Doan, and G. D. James, IAEA Sym-posium on the Physics and Chemistry of Fission, Jü-lich, 1979 (unpublished).
- ¹³W. Hauser and H. Feshbach, *Phys. Rev.* **87**, 366 (1952).
- ¹⁴P. A. Moldauer, *Nucl. Phys.* **47**, 65 (1963).
- ¹⁵H. M. Hofmann, J. Richert, J. W. Tepel, and H. A. Weidenmüller, *Ann. Phys. (N.Y.)* **90**, 403 (1975).
- ¹⁶W. K. Bertram, *Aust. J. Phys.* **31**, 151 (1978).
- ¹⁷J. M. Blatt and V. F. Weisskopf, *Theoretical Nuclear Physics* (Wiley, New York, 1952).
- ¹⁸J. D. Cramer and J. R. Nix, *Phys. Rev. C* **2**, 1048 (1970).
- ¹⁹R. W. Lamphere, *Nucl. Phys.* **38**, 561 (1962).
- ²⁰Ch. Lagrange, private communication.
- ²¹V. Metag, IAEA Symposium on the Physics and Chem-istry of Fission, Jülich, 1979 (unpublished).
- ²²J. E. Lynn, G. D. James, and L. G. Earwaker, AERE-Report No. R 6901 (1971).
- ²³I. Ragnarsson, S. G. Nilsson, and R. K. Sheline, *Phys. Rep.* **45**, 1 (1978), and private communication.
- ²⁴A. Bohr and B. R. Mottelson, *Nuclear Structure* (Ben-jamin, New York, 1975), Vol. 2.
- ²⁵J. W. Boldeman, A. R. de L. Musgrove, and R. L. Walsh, IAEA Symposium on the Physics and Chemistry of Fission, Jülich, 1979 (unpublished).
- ²⁶J. Blons *et al.*, private communication and the 18th International Winter Meeting on Nuclear Physics, Bor-mio, 1980 (unpublished).
- ²⁷H. C. Pauli and T. Ledergerber, in *Proceedings of the Third IAEA Symposium on the Physics and Chemistry of Fission, Rochester, 1973* (IAEA, Vienna, 1974), Vol. 1, p. 463.
- ²⁸M. Brack, Jens Damgaard, A. S. Jensen, H. C. Pauli, V. M. Strutinsky, and C. Y. Wong, *Rev. Mod. Phys.* **44**, 320 (1972).
- ²⁹P. E. Vorotnikov, S. M. Subrovina, G. A. Otroschenko, and V. A. Shigin, *Sov. J. Nucl. Phys.* **5**, 207 (1967).
- ³⁰B. S. Bhandari, *Phys. Rev. C* **19**, 1820 (1979).
- ³¹P. Bloch, J. W. Boldeman, G. Haouat, Y. Patin, J. Si-gaud, and J. Trochon, CEA report (unpublished).